Electromechanical Dampers for Vibration Control of Structures and Rotors

Andrea Tonoli, Nicola Amati and Mario Silvagni
Mechanics Department, Mechatronics Laboratory - Politecnico di Torino
Italy

To the memory of Pietro, a model student, a first- class engineer, a hero

1. Introduction

Viscoelastic and fluid film dampers are the main two categories of damping devices used for the vibration suppression in machines and mechanical structures. Although cost effective and of small size and weight, they are affected by several drawbacks: the need of elaborate tuning to compensate the effects of temperature and frequency, the ageing of the material and their passive nature that does not allow to modify their characteristics with the operating conditions. Active or semi-active electro-hydraulic systems have been developed to allow some forms of online tuning or adaptive behavior. More recently, electrorheological, (Ahn et al., 2002), (Vance & Ying, 2000) and magnetorheological (Vance & Ying, 2000) semi-active damping systems have shown attractive potentialities for the adaptation of the damping force to the operating conditions. However, electro-hydraulic, electrorheological, and magnetorheological devices cannot avoid some drawbacks related to the ageing of the fluid and to the tuning required for the compensation of the temperature and frequency effects.

Electromechanical dampers seem to be a valid alternative to viscoelastic and hydraulic ones due to, among the others: a) the absence of all fatigue and tribology issues motivated by the absence of contact, b) the small sensitivity to the operating conditions, c) the wide possibility of tuning even during operation, and d) the predictability of the behavior. The attractive potentialities of electromechanical damping systems have motivated a considerable research effort during the past decade. The target applications range from the field of rotating machines to that of vehicle suspensions.

Passive or semi-active eddy current dampers have a simpler architecture compared to active closed loop devices, thanks to the absence of power electronics and position sensors and are intrinsically not affected by instability problems due to the absence of a fast feedback loop. The simplified architecture guarantees more reliability and lower cost, but allows less flexibility and adaptability to the operating conditions. The working principle of eddy current dampers is based on the magnetic interaction generated by a magnetic flux linkage's variation in a conductor (Crandall et al., 1968), (Meisel, 1984). Such a variation may be generated using two different strategies:

Source: Vibration Control, Book edited by: Dr. Mickaël Lallart,
ISBN 978-953-307-117-6, pp. 380, September 2010, Sciyo, Croatia, downloaded from SCIYO.COM

- moving a conductor in a stationary magnetic field that is variable along the direction of the motion;
- changing the reluctance of a magnetic circuit whose flux is linked to the conductor.

In the first case, the eddy currents in the conductor interact with the magnetic field and generate Lorenz forces proportional to the relative velocity of the conductor itself. In (Graves et al., 2000) this kind of damper are defined as "motional" or "Lorentz" type. In the second case, the variation of the reluctance of the magnetic circuit produces a time variation of the magnetic flux. The flux variation induces a current in the voltage driven coil and, therefore, a dissipation of energy. This kind of dampers is defined in (Nagaya, 1984) as "transformer", or "reluctance" type.

The literature on eddy current dampers is mainly focused on the analysis of "motional" devices. Nagaya in (Nagaya, 1984) and (Nagaya & Karube, 1989) introduces an analytical approach to describe how damping forces can be exploited using monolithic plane conductors of various shapes. Karnopp and Margolis in (Karnopp, 1989) and (Karnopp et al., 1990) describe how "Lorentz" type eddy current dampers could be adopted as semi-active shock absorbers in automotive suspensions. The application of the same type of eddy current damper in the field of rotordynamics is described in (Kligerman & Gottlieb, 1998) and (Kligerman et al., 1998).

Being usually less efficient than "Lorentz" type, "transformer" eddy current dampers are less common in industrial applications. However they may be preferred in some areas for their flexibility and construction simplicity. If driven with a constant voltage they operate in passive mode while if current driven they become force actuators to be used in active configurations. A promising application of the "transformer" eddy current dampers seems to be their use in aero-engines as a non rotating damping device in series to a conventional rolling bearing that is connected to the main frame with a mechanical compliant support. Similarly to a squeeze film damper, the device acts on the non rotating part of the bearing. As it is not rotating, there are no eddy currents in it due to its rotation but just to its whirling. The coupling effects between the whirling motion and the torsional behavior of the rotor can be considered negligible in balanced rotors (Genta, 2004).

In principle the behaviour of Active Magnetic Dampers (AMDs) is similar to that of Active Magnetic Bearings (AMBs), with the only difference that the force generated by the actuator is not aimed to support the rotor but just to supply damping. The main advantages are that in the case of AMDs the actuators are smaller and the system is stable even in open-loop (Genta et al., 2006),(Genta et al., 2008),(Tonoli et al., 2008). This is true if the mechanical stiffness in parallel to the electromagnets is large enough to compensate the negative stiffness induced by the electromagnets.

Classical AMDs work according to the following principle: the gap between the rotor and the stator is measured by means of position sensors and this information is then used by the controller to regulate the current of the power amplifiers driving the magnet coils. Self-sensing AMDs can be classified as a particular case of magnetic dampers that allows to achieve the control of the system without the introduction of the position sensors. The information about the position is obtained by exploiting the reversibility of the electromechanical interaction between the stator and the rotor, which allows to obtain mechanical variables from electrical ones.

The sensorless configuration leads to many advantages during the design phase and during the practical realization of the device. The intrinsic punctual collocation of the not present sensor avoids the inversion of modal phase from actuator to sensor, with the related loss of

the zero/pole alternation and the consequent problems of stabilization that may affect a sensed solution. Additionally, getting rid of the sensors leads to a reduction of the costs, the reduction of the cabling and of the overall weight.
The aim of the present work is to present the experience of the authors in developing and testing several electromagnetic damping devices to be used for the vibration control.
A brief theoretical background on the basic principles of electromagnetic actuator, based on a simplified energy approach is provided. This allow a better understanding of the application of the electromagnetic theory to control the vibration of machines and mechanical structures. According to the theory basis, the modelling of the damping devices is proposed and the evidences of two dedicated test rigs are described.

2. Description and modelling of electromechanical dampers

2.1 Electromagnetic actuator basics

Electromagnetic actuators suitable to develop active/semi-active/passive damping efforts can be classified in two main categories: Maxwell devices and Lorentz devices.
For the first, the force is generated due to the variation of the reluctance of the magnetic circuit that produces a time variation of the magnetic flux linkage. In the second, the damping force derives from the interaction between the eddy currents generated in a conductor moving in a constant magnetic field.

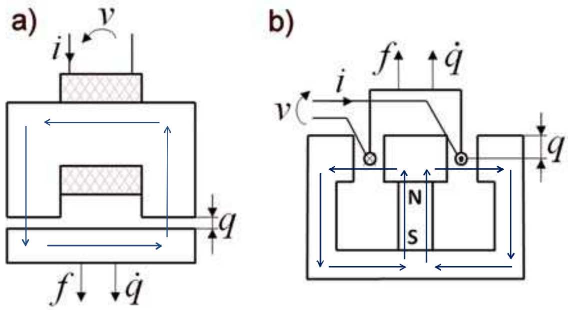

Fig. 1. Sketch of a) Maxwell magnetic actuator and b) Lorentz magnetic actuator.

For both (Figure 1), the energy stored in the electromagnetic circuit can be expressed by:

$$E = \int_{t_0}^{t_1} \left(P_{electrical} + P_{mechanical} \right) dt = \int_{t_0}^{t_1} \left(v(t)i(t) + f(t)\dot{q}(t) \right) dt \quad (1)$$

Where the electrical power ($P_{electrical}$) is the product of the voltage ($v(t)$) and the current ($i(t)$) flowing in the coil, and the mechanical power is the product of the force ($f(t)$) and speed ($\dot{q}(t)$) of the moving part of the actuator.
Considering the voltage ($v(t)$) as the time derivative of the magnetic flux linkage ($\lambda(t)$), eq.(1) can be written as:

$$E = \int_{t_0}^{t_1} \left(\frac{d\lambda(t)}{dt} i(t) + f(t)\dot{q}(t) \right) dt = \int_{\lambda_0}^{\lambda_1} i(t) d\lambda + \int_{q_0}^{q_1} f(t) dq = E_\lambda + E_q \quad (2)$$

In the following steps, the two terms of the energy E will be written in explicit form. With reference to Maxwell Actuator, Figure 1a, the Ampère law is:

$$H_a l_a + H_{fe} l_{fe} = Ni \tag{3}$$

where H_a and H_{fe} indicate the magnetic induction in the airgap and in the iron core while l_a and l_{fe} specify the length of the magnetic circuit flux lines in the airgap in the same circuit. The product Ni is the total current linking the magnetic flux (N indicates the number of turns while i is the current flowing in each wire section). If the magnetic circuit is designed to avoid saturation into the iron, the magnetic flux density B can be related to magnetic induction by the following expression:

$$B = \mu_0 H \quad , \quad B = \mu_0 \mu_{fe} H_{fe} . \tag{4}$$

Considering that ($\mu_{fe} >> \mu_0$) and noting that the total length of the magnetic flux lines in the airgap is twice q, eq.(3) can be simply written as:

$$\frac{2Bq}{\mu_0} = Ni . \tag{5}$$

The expressions of the magnetic flux linking a single turn and the total number of turns in the coil are respectively:

$$\varphi = BS_{airgap} \tag{6}$$

$$\lambda = N\varphi = NBS_{airgap} = \mu_0 \frac{N^2 S_{airgap}}{2q} i \tag{7}$$

Hence, knowing the expression (eq.(7)) of the total magnetic flux leakage, the E_λ of eq. (1) for a generic flux linkage λ and air q, can be computed as:

$$E_\lambda = \int_{\lambda_0}^{\lambda_1} i(t) d\lambda = \frac{\lambda^2 q}{\mu_0 N^2 S_{airgap}} \tag{8}$$

Note that this is the total contribution to the energy (E) if no external active force is applied to the moving part.
Finally, the force generated by the actuator and the current flowing into the coil can be computed as:

$$f = \frac{\partial E}{\partial q} = \frac{\lambda^2}{\mu_0 N^2 S_{airgap}} , \tag{9}$$

$$i = \frac{\partial E}{\partial \lambda} = \frac{2q\lambda}{\mu_0 N^2 S_{airgap}} . \tag{10}$$

Then, the force relative to the current can be obtained by substituting eq.(10) into eq.(9):

$$f = \frac{\mu_0 N^2 S_{airgap} i^2}{4q^2} . \qquad (11)$$

Considering the **Lorentz actuator** (Figure 1 b**)**, if the coil movement q is driven while the same coil is in open circuit configuration so that no current flows in the coil, the energy (*E*) is zero as both the integrals in eq. (1) are null. In the case the coil is in a constant position and the current flow in it varies from zero to a certain value, the contribution of the integral leading to (E_q) is null as the displacement of the anchor (*q*) is constant while the integral leading to (E_λ) can be computed considering the total flux leakage.

$$\lambda = 2\pi RqB + Li = \lambda_0 + Li \qquad (12)$$

The first term is the contribution of the magnetic circuit (R is the radius of the coil, q is the part of the coil in the magnetic field), while the second term is the contribution to the flux of the current flowing into the coil. Current can be obtained from eq.(12) as:

$$i = \frac{\lambda - \lambda_0}{L} \qquad (13)$$

Hence, from the expression of eq.(13), the E_λ term, that is equal to the total energy, can be computed as:

$$E_\lambda = \int_{\lambda_0}^{\lambda_1} i(t) d\lambda = \int_{\lambda_0}^{\lambda_1} \frac{\lambda - \lambda_0}{L} d\lambda = \frac{1}{2L}(\lambda - \lambda_0)^2 = \frac{1}{2L}(\lambda - 2\pi RqB)^2 \qquad (14)$$

Finally computing the derivative with respect to the displacement and to the flux, the force generated by the actuator and the current flowing into the coil can be computed:

$$f = \frac{\partial E}{\partial q} = \frac{-2\pi RB}{L}(\lambda - \lambda_0) \qquad (15)$$

$$i = \frac{\partial E}{\partial \lambda} = \frac{1}{L}(\lambda - \lambda_0) \qquad (16)$$

The expression of the force relative to the current can be obtained by substituting eq.(16) into eq.(15)

$$f = -2\pi RBi . \qquad (17)$$

The equations above mentioned represent the basis to understand the behaviour of electromagnetic actuators adopted to damp the vibration of structures and machines.

2.2 Classification of electromagnetic dampers

Figure 2 shows a sketch representing the application of a Maxwell type and a Lorentz type actuator. In the field of damping systems the former is named transformer damper while the latter is called motional damper. The transformer type dampers can operate in active mode if current driven or in passive mode if voltage driven. The drawings evidence a compliant supporting device working in parallel to the damper. In the specific its role is to support the weight of the rotor and supply the requested compliance to exploit the performance of the damper (Genta, 2004). Note that the sketches are referred to an application for rotating systems. The aim in this case is to damp the lateral vibration of the rotating part but the concept can be extended to any vibrating device. In fact, the damper interacts with the non rotating raceway of the bearing that is subject only to radial vibration motion.

2.3 Motional eddy current dampers

The present section is devoted to describe the equations governig the behavior of the motional eddy current dampers. A torsional device is used as reference being the linear ones a subset. The reference scheme (Kamerbeek, 1973) is a simplified induction motor with one magnetic pole pair (Figure 3a).

The rotor is made by two windings 1,1′ and 2,2′ installed in orthogonal planes. It is crossed by the constant magnetic field (flux density $\mathbf{B}_s$) generated by the stator. The analysis is performed under the following assumptions:

- the two rotor coils have the same electric parameters and are shorted.
- The reluctance of the magnetic circuit is constant. The analysis is therefore only applicable to motional eddy current devices and not to transformer ones (Graves et al., 2009), (Tonoli et al., 2008).

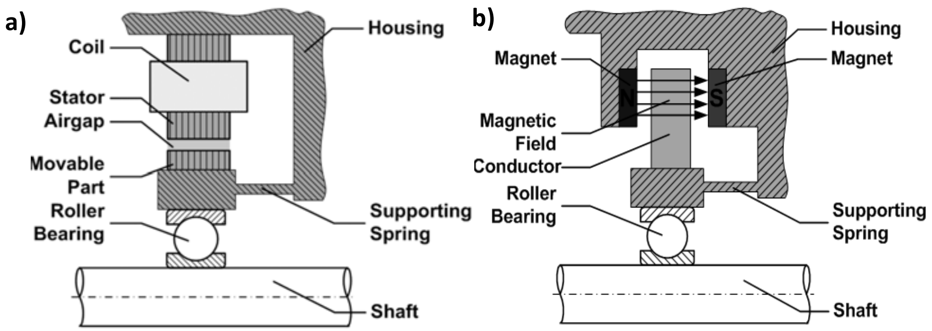

Fig. 2. Sketch of a transformer (a) and a motional damper (b).

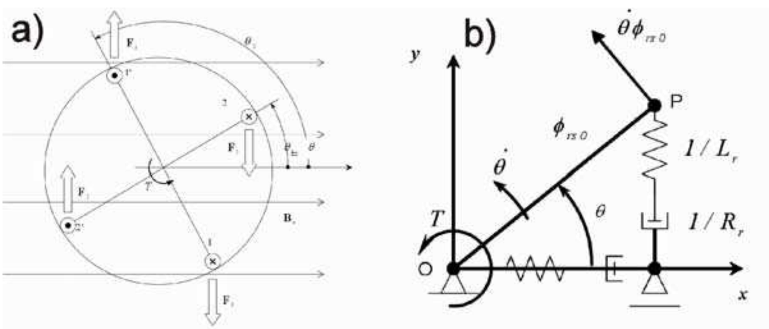

Fig. 3. a) Sketch of the induction machine b) Mechanical analogue. The torque T is balanced by the force applied to point P by the spring-damper assemblies.

- The magnetic flux generated by the stator is constant as if it were produced by permanent magnets or by current driven electromagnets.
- The stator is assumed to be fixed. This is equivalent to describe the system in a reference frame rigidly connected to it.
- All quantities are assumed to be independent from the axial coordinate.
- Each of the electric parameter is assumed to be lumped.

Angle $\theta(t)$ between the plane of winding 2 and the direction of the magnetic field indicates the angular position of the rotor relative to the stator. When currents i_{r1} and i_{r2} flow in the windings, they interact with the magnetic field of the stator and generate a pair of Lorentz forces ($F_{1,2}$ in Figure 3a). Each force is perpendicular to both the magnetic field and to the axis of the conductors. They are expressed as:

$$F_1 = Nl_r i_{r1} B_s, \qquad F_2 = Nl_r i_{r2} B_s \tag{18}$$

where N and l_r indicate the number of turns in each winding and their axial length. The resulting electromagnetic torques T_1 and T_2 applied to the rotor of diameter d_r are:

$$T_1 = F_1 d_r \sin\theta = \phi_{rs0} \sin\theta\, i_{r1}, \qquad T_2 = F_2 d_r \cos\theta = \phi_{rs0} \cos\theta\, i_{r2} \tag{19}$$

where $\phi_{rs0} = Nl_r d_r B_s$ is the magnetic flux linked with each coil when its normal is aligned with the magnetic field $\mathbf{B}_s$. It represents the maximum magnetic flux. The total torque acting on the rotor is:

$$T = T_1 + T_2 = \phi_{rs0}\left(\sin\theta\, i_{r1} + \cos\theta\, i_{r2}\right) \tag{20}$$

Note that the positive orientation of the currents indicated in Figure 3a has been assumed arbitrarily, the results are not affected by this choice.

From the mechanical point of view the eddy current damper behaves then as a crank of radius ϕ_{rs0} whose end is connected to two spring/damper series acting along orthogonal directions. Even if the very concept of mechanical analogue is usually a matter of elementary physics textbooks, the mechanical analogue of a torsional eddy current device is not common in the literature. It has been reported here due to its practical relevance. Springs and viscous dampers can in fact be easily assembled in most mechanical simulation environments. The mechanical analogue in Figure 3b allows to model the effect of the eddy current damper without needing a multi-domain simulation tool.

The model of an eddy current device with p pole pairs can be obtained by considering that each pair involves two windings electrically excited with 90º phase shift. For a one pole pair device, each pair is associated with a rotor angle of 2π rad; a complete revolution of the rotor induces one electric excitation cycle of its two windings. Similarly, for a p pole pairs device, each pair is associated to a $2\pi / p$ rad angle, a complete revolution of the rotor induces then p excitation cycles on each winding ($\theta_e = p\theta$).

The orthogonality between the two windings allows adopting a complex flux linkage variable

$$\phi_r = \phi_{r1} + j\phi_{r2} \tag{21}$$

where j is the imaginary unit. Similarly, also the current flowing in the windings can be written as $i_r = i_{r1} + ji_{r2}$. The total magnetic flux ϕ_r linked by each coil is contributed by the currents i_r through the self inductance L_r and the flux generated by the stator and linked to the rotor

$$\phi_r = L_r i_r + \frac{\phi_{rs0}}{p} e^{-j\theta_e} . \tag{22}$$

The differential equation governing the complex flux linkage ϕ_r is obtained by substituting eq.(22) in the Kirchoff's voltage law

$$\frac{d\phi_r}{dt} + R_r i_r = 0 . \tag{23}$$

It is therefore expressed as

$$\dot{\phi}_r + \omega_p \phi_r = j\dot{\theta}\phi_{rs0} e^{-j\theta_e} \tag{24}$$

where ω_p is the is the electrical pole of each winding

$$\omega_p = \frac{R_r}{L_r} . \tag{25}$$

The electromagnetic torque of eq.(20) results to be p times that of a single pole pair

$$T = p \frac{\phi_{rs0}}{L_r} Im\left(\phi_r e^{j\theta_e}\right) . \tag{26}$$

The model holds under rather general input angular speed. The mechanical torque will be determined for the following operating conditions:

- coupler: the angular speed is constant: $\dot{\theta} = \Omega = \text{const}$,
- damper: the rotor is subject to a small amplitude torsional vibration relative to the stator.

Coupler

For constant rotating speed ($\dot{\theta}(t) = \Omega$, $\theta(t) = \Omega t$), the steady state solution of eq.(24) is

$$\phi_r = \phi_{r0} e^{-jp\Omega t}; \qquad \phi_{r0} = \frac{j\Omega\phi_{rs0}}{\omega_p - jp\Omega} \tag{27}$$

The torque (T) to speed (Ω) characteristic is found by substituting eq.(27) into eq.(26). The result is the familiar torque to slip speed expression of an induction machine running at constant speed

$$T(\Omega) = \frac{c_0}{1 + (p\Omega)^2 / \omega_p^2} \Omega, \qquad \text{where } c_0 = \frac{p\phi_{rs0}^2}{R_r} . \tag{28}$$

A simple understanding of this characteristic can be obtained by referring to the mechanical analogue of Figure 3b. At speeds such that the excitation frequency is lower than the pole ($p\Omega << \omega_p$), the main contribution to the deformation is that of the dampers, while the springs behave as rigid bodies. The resultant force vector acting on point P is due to the dampers and acts perpendicularly to the crank ϕ_{rs0}, this produces a counteracting torque

$$T = c_0\Omega \tag{29}$$

By converse, at speeds such that $p\Omega >> \omega_p$ the main contribution to the deformation is that of the springs, while the dampers behave as rigid bodies. The resultant force vector on point P is due to the springs. It is oriented along the crank ϕ_{rs0} and generates a null torque.

Damper

If the rotor oscillates ($\theta(t) = \theta_0 \Re e(e^{j\omega t}) + \theta_m$) with small amplitude about a given angular position θ_m, the state eq.(24) can be linearized resorting to the small angle assumption

$$\dot{\phi}_r + \omega_p \phi_r = j\dot{\theta}\phi_{rs0}e^{-jp\theta_m} \tag{30}$$

The solution is found in terms of the transfer function between the rotor flux $\phi_r(s)$ and the input speed $\dot{\theta}(s)$

$$\frac{\phi_r(s)}{\dot{\theta}(s)} = \frac{j\phi_{rs0}e^{-jp\theta_m}}{s+\omega_p}, \tag{31}$$

where s is the Laplace variable. The mechanical impedance $Z_m(s)$, i.e. the torque to speed transfer function is found by substituting eq.(31) into Eq.(26)

$$Z_m(s) = \frac{T(s)}{\dot{\theta}(s)} = \frac{c_{em}}{1+s/\omega_p} = \frac{c_{em}}{1+s\left(k_{em}/c_{em}\right)}. \tag{32}$$

This impedance is that of the series connection of a torsional damper and a torsional spring with viscous damping and spring stiffness given by

$$c_{em} = \frac{p\phi_{rs0}^2}{R_r}, \qquad k_{em} = \frac{p\phi_{rs0}^2}{L_r} \tag{33}$$

that are constant parameters. At low frequency ($s << \omega_p$), the device behaves as a pure viscous damper with coefficient c_{em}. This is the term that is taken into account in the widespread reactive model. At high frequency ($s >> \omega_p$) it behaves as a mechanical linear spring with stiffness k_{em}. This term on the contrary is commonly neglected in all the models presented in the literature (Graves et al., 2009), (Nagaya, 1984), (Nagaya & Karube, 1989). The bandwidth of the mechanical impedance (Figure 4b) is due to the electrical circuit resistance and inductance. It must be taken into account for the design of eddy current dampers. The assumption of neglecting the inductance is valid only for frequency lower than the electric pole ($s << \omega_p$). The behavior of the mechanical impedance has effects also on the operation of an eddy current coupler. Due to the bandwidth limitations, it behaves as a low pass filter for each frequency higher than the electric pole.
To correlated the torque to speed characteristic of eq.(28) and the mechanical impedance of eq.(32), it shold be analized that the slope c_0 of the torque to speed characteristic at zero or low speed ($\Omega = p\omega_p$) is equal to the mechanical impedance at zero or low frequency ($s = \omega_p$):

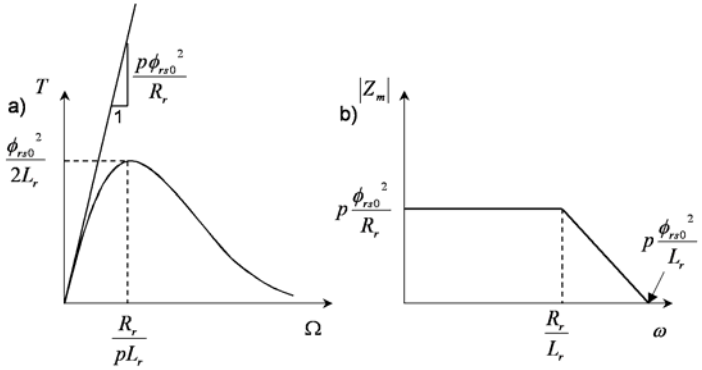

Fig. 4. a) Static characteristic of an axial-symmetric induction machine b) Representation of its mechanical impedance (magnitude in logarithmic scales).

$$c_0 = c_{em} = \frac{p\phi_{rs0}^2}{R_r}. \tag{34}$$

Additionally, the maximum torque ($T_{\max}$) at steady state is related to the high frequency mechanical impedance ($Z_m(s)$)

$$T_{\max} = \frac{\phi_{rs0}^2}{2L_r},\ k_{em} = \frac{p\phi_{rs0}^2}{L_r} \tag{35}$$

The relationship between $T_{\max}$ and $Z_m(s)$ at high frequency is therefore

$$\Omega_{T_{\max}} = \frac{\omega_p}{p}, \qquad T_{\max} = \frac{c_{em}\omega_p}{2p} = \frac{k_{em}}{2p} \tag{36}$$

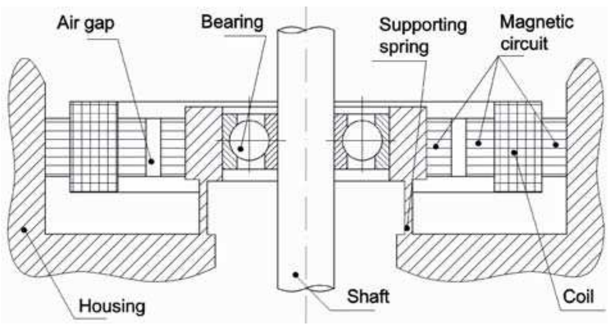

Fig. 5. Sketch of an Active Magnetic Damper in conjunction with a mechanical spring. They both act on the non rotating part of the bearing.

A graphical representation of the relationships between eqs.(35) and (36) is given in Figure 4. They allow to obtain the mechanical impedance and/or the state space model valid under general operating condition, eq.(24), from the torque to speed characteristic. This is of

interest because numerical tools performing constant speed analysis are far more common and consolidated than those dealing with transient analysis. Vice versa, the steady state torque to speed characteristic can be simply obtained identifying by vibration tests the parameters c_{em} and k_{em} (or ω_p).
It's worth to note that eqs.(28), (32) and Eqs.(35), (36) hold in general for eddy current devices with one or more pole pairs. They can be applied also to linear electric machies provided that the rotational degree of freedom is transformed into a linear one.

2.4 Transformer dampers in active mode (AMD)

Transformer dampers can be used in active mode. Active Magnetic Dampers (Figure 5) work in the same way as active magnetic bearings, with the only difference that in this case the force generated by the actuator is not aimed to support the rotor but, in the simplest control strategy, it may be designed just to supply damping; this doesn't exclude the possibility to develop any more complex control strategy. An AMD can be integrated into one of the supports of the rotor. In this concept, a rolling element bearing is supported in the housing via mechanical springs providing the required stiffness. Both the spring and the damper act on the non-rotating part of the support. The stiffness and the load bearing capacity is then provided by the mechanical device while the AMD is used to control the vibrations, adding damping, in its simplest form. It is important to note that the stiffness of the springs can be used to compensate the open loop negative stiffness of a typical Maxwell actuator. This allows to relieve the active control of the task to guarantee the static stability of the system. A proportional-derivative feedback loop based on the measurement of the support displacements may be enough to control the rotor vibrations. Sensors and a controller are then required to this end. Under the assumption of typical Maxwell actuators, the force that each coil of the actuator exerts on the moving part is computed by eq.(11), that can be used to design the actuators once its maximum control force is specified. It's worth to note that such damping devices can be applied to any vibrating system.

2.5 Transformer dampers in active mode and self-sensing operation

The reversibility of the electromechanical interaction induces an electrical effect when the two parts of an electromagnet are subject to relative motion (back electromotive force). This effect can be exploited to estimate mechanical variables from the measurement of electrical ones. This leads to the so-called self-sensing configuration that consists in using the electromagnet either as an actuator and a sensor. This configuration permits lower costs and shorter shafts (and thus higher bending frequencies) than classical configurations provided with sensors and non-collocation issues are avoided. In practice, voltage and current are used to estimate the airgap. To do so, the two main approaches are: the state-space observer approach (Vischer & Bleuler, 1990), (Vischer & Bleuler, 1993) and the airgap estimation using the current ripple (Noh & Maslen, 1997), (Schammass et al., 2005). The former is based on the electromechanical model of the system. As the resulting model is fully observable and controllable, the position and the velocity of the mechanical part can be estimated and fed back to control the vibrations of the system. This approach is applicable for voltage-controlled (Mizuno et al., 1996) and current-controlled (Mizuno et al., 1996) electromagnets. The second approach takes advantage from the current ripple due to the switching amplifiers to compute in real-time the inductance, and thus the airgap. The airgap-estimation can be based on the ripple slope (PWM driven amplifiers, (Okada et al., 1992)) or on the ripple frequency (hysteresis amplifiers, (Mizuno et al., 1998)). So far in the literature, self-sensing configurations have been mainly used to achieve the complete suspension of the rotor. The poor robustness of the state-space approach greatly limited its adoption for industrial applications. As a matter of fact, the use of a not well tuned model results in the system instability (Mizuno et al., 1996) , (Thibeault & Smith 2002). Instead, the direct airgap estimation approach seems to be more promising in terms of robustness (Maslen et al., 2006).

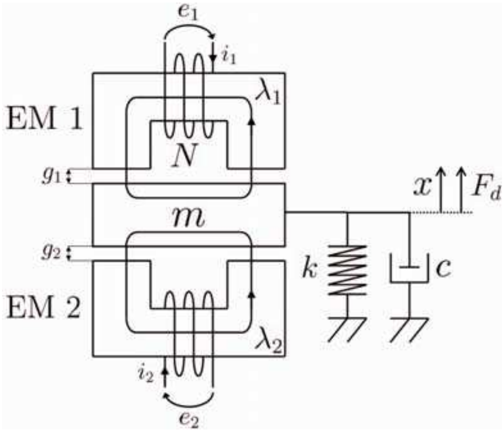

Fig. 6. Schematic model of electromagnets pair to be used for self-sensing modelling.

Here below is described a one degree of freedom mass-spring oscillator actuated by two opposite electromagnets (Figure 6). Parameters *m*, *k* and *c* are the mass, stiffness and viscous damping coefficient of the mechanical system. The electromagnets are assumed to be identical, and the coupling between the two electromagnetic circuits is neglected. The aim of the mechanical stiffness is to compensate the negative stiffness due to the electromagnets.
Owing to Newton's law in the mechanical domain, the Faraday and Kirchoff laws in the electrical domain, the dynamics equations of the system are:

$$\begin{aligned} m\ddot{x} + c\dot{x} + kx + F_1 + F_2 &= F_d \\ \dot{\lambda}_1 + Ri_1 &= v_1 \\ \dot{\lambda}_2 + Ri_2 &= v_2 \end{aligned} \tag{37}$$

where R is the coils resistance and v_j is the voltage applied to electromagnet j. F_d is the disturbance force applied to the mass, while F_1 and F_2 are the forces generated by the coils as in eq. (9).
The system dynamics is linearized around a working point corresponding to a bias voltage v_0 imposed to both the electromagnets:

$$\begin{aligned} i_j &= i_0 \pm i_c \\ v_j &= v_0 \pm v_c\,, j = 1,2 \\ F_j\left(i_j, x\right) &= \pm F_0 + \Delta F_j \end{aligned} \tag{38}$$

where F_0 is the initial force generated by the electromagnets due to the current $i_0 = v_0 / R$, and ΔF_j is the small variation of the electromagnets' forces. As the electromagnets are identical, $(i_1 - i_0) = -(i_2 - i_0) = i_c$. Therefore, a three-state-space model is used to study the four-state system dynamics described in eq.(37) (Vischer & Bleuler, 1990). The resulting linearized state-space model is:

$$\begin{aligned} X &= AX + Bu \\ y &= CX \end{aligned} \tag{39}$$

where A, B and C are the dynamic, action and output matrices respectively defined as:

$$A = \begin{bmatrix} 0 & 1 & 0 \\ -\dfrac{k+2k_x}{m} & -\dfrac{c}{m} & \dfrac{2k_i}{m} \\ 0 & -\dfrac{k_m}{L_0} & -\dfrac{R}{L_0} \end{bmatrix},$$

$$B = \begin{bmatrix} 0 & 0 \\ \dfrac{1}{m} & 0 \\ 0 & \dfrac{1}{L_0} \end{bmatrix}, C = \begin{bmatrix} 0 & 0 & 1 \end{bmatrix}, \tag{40}$$

with the associated state, input and output vectors $X = \{x, \dot{x}, i_c\}^T$, $u = \{F_d, v_c\}^T$ $y = i_c$.
The terms in the matrices derive from the linearization of the non-linear functions defined in eq. (7) and eq. (9):

$$\begin{aligned} L_0 = \frac{\Gamma}{x_0}, \quad k_m = L_0 \frac{i_0}{x_0}, \\ k_i = L_0 \frac{i_0}{x_0}, \quad k_x = -k_m \frac{i_0}{x_0} \end{aligned}, \tag{41}$$

where $\Gamma = \mu_0 N^2 S / 2$ is the characteristic factor of the electromagnets , L_0, k_i, k_m and k_x are the inductance, the current-force factor, the back-electromotive force factor, and the so-called negative stiffness of one electromagnet, respectively. The open-loop system is stable as long as the mechanical stiffness is larger than the total negative stiffness, i.e. $k + 2k_x > 0$.
As eq.(39) describes the open-loop dynamics of the system for small variations of the variables, and the system stability is insured, the various coefficients of A can be identified experimentally.
Due to the strong nonlinearity of the electromagnetic force as a function of the displacement and the applied voltage, and to the presence of end stops that limit the travel of the moving

mass, the linear approach may seem to be questionable. Nevertheless, the presence of a mechanical stiffness large enough to overcome the negative stiffness of the electromagnets makes the linearization point stable, and compels the system to oscillate about it. The selection of a suitable value of the stiffness k is a trade-off issue deriving from the application requirements. However, as far as the linearization is concerned, the larger is the stiffness k relative to $|k_x|$, the more negligible the nonlinear effects become.

2.5.1 Control design

The aim of the present section is to describe the design strategy of the controller that has been used to introduce active magnetic damping into the system. The control is based on the Luenberger observer approach (Vischer & Bleuler, 1993), (Mizuno et al., 1996). The adoption of this approach was motivated by the relatively low level of noise affecting the current measurement. It consists in estimating in real time the unmeasured states (in our case, displacement and velocity) from the processing of the measurable states (the current). The observer is based on the linearized model presented previously, and therefore the higher frequency modes of the mechanical system have not been taken into account. Afterwards, the same model is used for the design of the state-feedback controller.

2.5.2 State observer

The observer dynamics is expressed as (Luenberger, 1971):

$$\dot{\hat{X}} = A\dot{X} + Bu + L\left(y - \hat{y}\right) \tag{42}$$

where $\hat{X}$ and $\hat{y}$ are the estimations of the system state and output, respectively. Matrix L is commonly referred to as the gain matrix of the observer. Eq.(42) shows that the inputs of the observer are the measurement of the current (y) and the control voltage imposed to the electromagnets (u).
The dynamics of the estimation error ε are obtained combining eq. (39) and eq. (42):

$$\dot{\varepsilon} = \left(A - LC\right)\varepsilon \tag{43}$$

where $\varepsilon = X - \hat{X}$. Eq. (43) emphasizes the role of L in the observer convergence. The location of the eigenvalues of matrix $\left(A - LC\right)$ on the complex plane determines the estimation time constants of the observer: the deeper they are in the left-half part of the complex plane, the faster will be the observer. It is well known that the observer tuning is a trade-off between the convergence speed and the noise rejection (Luenberger, 1971). A fast observer is desirable to increase the frequency bandwidth of the controller action. Nevertheless, this configuration corresponds to high values of L gains, which would result in the amplification of the unavoidable measurement noise y, and its transmission into the state estimation. This issue is especially relevant when switching amplifiers are used. Moreover, the transfer function that results from a fast observer requires large sampling frequencies, which is not always compatible with low cost applications.

2.5.3 State-feedback controller

A state-feedback control is used to introduce damping into the system. The control voltage is computed as a linear combination of the states estimated by the observer, with K as the control gain matrix. Owing to the separation principle, the state-feedback controller is designed considering the eigenvalues of matrix (A-BK).

Similarly to the observer, a pole placement technique has been used to compute the gains of K, so as to maintain the mechanical frequency constant. By doing so, the power consumption for damping is minimized, as the controller does not work against the mechanical stiffness. The idea of the design was to increase damping by shifting the complex poles closer to the real axis while keeping constant their distance to the origin ($|p_1| = |p_2| = constant$).

2.6 Semi-active transformer damper

Figure 7 shows the sketch of a "transformer" eddy current damper including two electromagnets. The coils are supplied with a constant voltage and generate the magnetic field linked to the moving element (anchor). The displacement with speed $\dot{q}$ of the anchor changes the reluctance of the magnetic circuit and produces a variation of the flux linkage. According to Faraday's law, the time variation of the flux generates a back electromotive force. Eddy currents are thus generated in the coils. The current in the coils is then given by two contributions: a fixed one due to the voltage supply and a variable one induced by the back electromotive force. The first contribution generates a force that increases with the decreasing of the air-gap. It is then responsible of a negative stiffness. The damping force is generated by the second contribution that acts against the speed of the moving element.

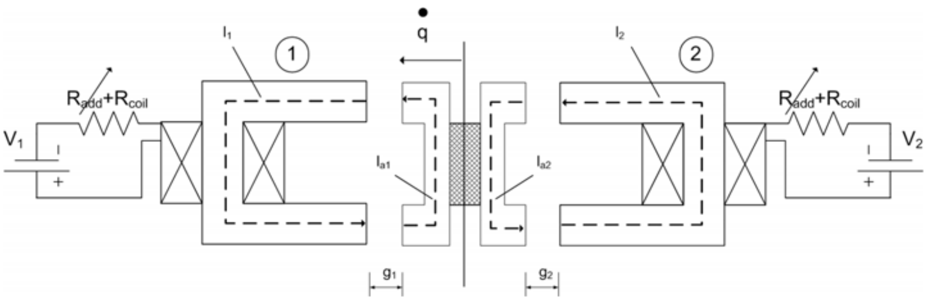

Fig. 7. Sketch of a two electromagnet Semi Active Magnetic Damper (the elastic support is omitted).

According to eq. (9), considering the two magnetic flux linkages λ_1 and λ_2 of both counteracting magnetic circuits, the total force acting on the anchor of the system is:

$$f = \frac{\lambda_2^2 - \lambda_1^2}{\mu_0 N^2 S_{airgap}} \tag{44}$$

The state equation relative to the electric circuit can be derived considering a constant voltage supply common for both the circuits that drive the derivative of the flux leakage and the voltage drop on the total resistance of each circuit R=R_{coil}+R_{add} (coil resistance and additional resistance used to tune the electrical circuit pole as:

$$\dot{\lambda}_1 + \alpha R\left(g_0 - q\right)\lambda_1 = V$$
$$\dot{\lambda}_2 + \alpha R\left(g_0 + q\right)\lambda_2 = V \tag{45}$$

Where g_0 is the nominal airgap and $\alpha = 2/(\mu_0 N^2 A)$.
Eqs.(44) and (45) are linearized for small displacements about the centered position of the anchor ($q = 0$) to understand the system behavior in terms of poles and zero structure

$$\dot{q} = v,$$
$$\dot{\lambda}_1' = -\alpha R\left(g_0\lambda_1' - \lambda_0 q\right),$$
$$\dot{\lambda}_2' = -\alpha R\left(g_0\lambda_2' + \lambda_0 q\right), \tag{46}$$

$$F_{em} = \alpha\lambda_0\left(\lambda_2' - \lambda_1'\right). \tag{47}$$

The term $\lambda_0 = V/\left(\alpha g_0 R\right)$ represents the magnetic flux linkage in the two electromagnets at steady state in the centered position as obtained from eq.(45) while λ_1' and λ_2' indicate the variation of the magnetic flux linkages relative to λ_0 .
The transfer function between the speed $\dot{q}$ and the electromagnetic force F shows a first order dynamic with the pole (ω_{RL}) due to the R-L nature of the circuits

$$\frac{F_{em}}{\dot{q}} = \frac{1}{s}\frac{K_{em}}{\left(1 + s/\omega_{RL}\right)},$$
$$\left(K_{em} = -\frac{2V^2/R}{g_0^2\omega_{RL}}, \quad \omega_{RL} = \frac{R}{L_0}, \; L_0 = \frac{\mu_0 N^2 A}{2g_0}\right). \tag{48}$$

L_0 indicates the inductance of each electromagnet at nominal airgap.
The mechanical impedance is a band limited negative stiffness. This is due to the factor $1/s$ and the negative value of K_{em} that is proportional to the electrical power ($K_m \geq -K_{em}$) dissipated at steady state by the electromagnet.
The mechanical impedance and the pole frequency are functions of the voltage supply V and the resistance R whenever the turns of the windings (N), the air gap area (A) and the airgap (g_0) have been defined. The negative stiffness prevents the use of the electromagnet as support of a mechanical structure unless the excitation voltage is driven by an active feedback that compensates it. This is the principle at the base of active magnetic suspensions.
A very simple alternative to the active feedback is to put a mechanical spring in parallel to the electromagnet. In order to avoid the static instability, the stiffness K_m of the added spring has to be larger than the negative electromechanical stiffness of the damper ($K_m \geq -K_{em}$). The mechanical stiffness could be that of the structure in the case of an already supported structure. Alternatively, if the structure is supported by the dampers themselves, the springs have to be installed in parallel to them. As a matter of fact, the mechanical spring in parallel to the transformer damper can be considered as part of the damper.

Due to the essential role of that spring, the impedance of eq.(48) is not very helpful in understanding the behavior of the damper. Instead, a better insight can be obtained by studying the mechanical impedance of the damper in parallel to the mechanical spring:

$$\frac{F_{em}}{v} = \frac{1}{s}\left(\frac{K_{em}}{\left(1+s/\omega_{RL}\right)} + K_m\right) = \frac{K_{eq}}{s}\frac{1+s/\omega_z}{1+s/\omega_{RL}}$$
$$\text{where } K_{eq} = K_m + K_{em}\,;\ \omega_z = \omega_{RL}\frac{K_{eq}}{K_m}\,. \tag{49}$$

Apart from the pole at null frequency, the impedance shows a zero-pole behavior. To ensure stability ($0 < -K_{em} < K_m$), the zero frequency (ω_z) results to be smaller than the pole frequency ($0 < \omega_z < \omega_{RL}$).

Figure 8a underlines that it is possible to identify three different frequency ranges:

1. Equivalent stiffness range ($\omega << \omega_z < \omega_{RL}$): the system behaves as a spring of stiffness $K_{eq} > 0$.
2. Damping range ($\omega_z < \omega < \omega_{RL}$): the system behaves as a viscous damper of coefficient

$$C = \frac{K_m}{\omega_{RL}} \tag{50}$$

3. Mechanical stiffness range ($\omega_z < \omega_{RL} << \omega$): the transformer damper contribution vanishes and the only contribution is that of the mechanical spring (K_m) in series to it.

A purely mechanical equivalent of the damper is shown in Figure 8b where a spring of stiffness K_{eq} is in parallel to the series of a viscous damper of coefficient *C* and a spring of stiffness $-K_{em}$. Due to the negative value of the electromagnetic stiffness, $-K_{em}$ is positive. It is interesting to note that the resulting model is the same as Maxwell's model of viscoelastic materials. At low frequency the system is dominated by the spring K_{eq} while the lower branch of the parallel connection does not contribute. At high frequency the viscous damper "locks" and the stiffnesses of the two springs add. The viscous damping dominates in the intermediate frequency range.

Eq. (50) shows that the product of the damping coefficient *C* and the pole frequency ω_{RL} is equal to the mechanical spring stiffness K_m. A sort of constant gain-bandwidth product therefore characterizes the damping range of the electromechanical damper. This product is just a function of the spring stiffness included in the damper. The constant gain-bandwidth means that for a given electromagnet, an increment of the added resistance leads to a higher pole frequency (eq. (48)) but reduces the damping coefficient of the same amount. Another interesting feature of the mechanical impedance of eq. (49) is that the only parameters affected by the supply voltage *V* are the equivalent stiffness (K_{eq}) and the zero-frequency (ω_z). The damping coefficient (*C*) and the pole frequency (ω_{RL}) are independent of it.

The substitution of the electromechanical stiffness K_{em} of eq. (48) into eq. (49) gives the zero frequency as function of the excitation voltage

$$\omega_z = \omega_{RL}\left(1 - \frac{2V^2/R}{g_0^2\omega_{RL}K_m}\right). \tag{51}$$